Rev. Lett. 29, 211 (1972).

[2] I. Rudnick and J. C. Fraser, J. Low Temp. Phys. 3, 225 (1970); J. H. Scholtz, E. O. McLean, and I. Rudnick, Phys. Rev. Lett. 32, 147 (1974).

[3] R. P. Henkel, G. Kukich, and J. D. Reppy, in *Proceedings of the Eleventh International Conference on Low Temperature Physics, St. Andrews, Scotland, 1968,* edited by J. F. Allen, D. M. Finlayson, and D. M. McCall (St. Andrews Univ. Press, St. Andrews, Scotland, 1969); H. W. Chan, A. W. Yanof, F. D. Pobell, and J. D. Reppy, in *Low Temperature Physics, LT-13,* edited by W. J. O'Sullivan, K. D. Timmerhaus, and E. F. Hammel (Plenum, New York, 1973).

[4] V. L. Ginzburg and L. P. Pitaevskii, Zh. Eksp. Teor. Fiz. 34, 1240 (1958) [Sov. Phys. JETP 34, 858 (1958)].

[5] E. P. Gross, J. Math. Phys. (N. Y.) 4, 195 (1963).

[6] Yu. G. Mamaladze, Zh. Eksp. Teor. Fiz. 52, 729 (1967) [Sov. Phys. JETP 25, 479 (1967)].

[7] J. G. Dash and J. A. Herb, Phys. Rev. A 7, 1427 (1973).

[8] M. W. Cole, J. G. Dash, and J. A. Herb, Phys. Rev. B 11, 163 (1975).

[9] When $l \approx \lambda_3$, the third-sound wavelength, the superfluid may oscillate as a standing wave with its center of mass moving further than that of the crystal. In this case, the contained fluid can contribute more (or less) to Δf than just its normal mass. The average effect over the entire crystal depends on the distribution of the sizes and shapes of the irregularities and the third-sound attenuation. This nonlinear contribution could affect the shapes and magnitudes of the curves in Figs. 2 and 3, but its contribution depends on little-known parameters and is very difficult to calculate.

[10] Hewlett Packard 5100A Frequency Synthesizer driven by a Hewlett Packard 5110A Synthesizer Driver.

[11] International Crystal Mfg. Co., 10 North Lee, Oklahoma City, Okla. 73102.

[12] Although the crystal environment was the same at 8 and 24 MHz, the film thicknesses were not identical. Since onset at 8 MHz occurred at lower T, the pressure was correspondingly lower and the film thicker which enhances the frequency shift.

[13] B. Ratnan and J. Mochel, J. Low Temp. Phys. 3, 239 (1970).

[14] We estimate $\Delta T_0 = 0$ at about $n = 7.5$ layers from the Frenkel-Halsey-Hill expression $n = [\alpha (T \ln p_0/p)^{-1}]^{1/3}$ where p/p_0 is the relative vapor pressure at temperature T and α is a measure of Van der Waals' attraction between the helium and the substrate. See D. M. Young and A. D. Crowell, *Physical Adsorption of Gases* (Butterworths, London, 1962). Since α could not be experimentally determined for our substrate, we employed $\alpha = 39$ (layer)^3 K from Ref. 1.

[15] J. S. Langer and M. E. Fisher, Phys. Rev. Lett. 19, 560 (1967). See also J. S. Langer and J. D. Reppy, in *Progress in Low Temperature Physics,* edited by C. J. Gorter (North-Holland, Amsterdam, 1970), Vol. 6, Chap. 1.

[16] In this experiment, the superfluid velocity is taken to be the relative velocity between the superfluid and the crystal surface and hence the velocity of the surface due to the applied electric field. Using the work of C. D. Stockbridge, in *Vacuum Microbalance Techniques,* edited by K. H. Behrndt (Plenum, New York, 1966), Vol. 5, pp. 161–167, we estimate the surface velocity of the crystal at the third overtone to be approximately twice that of the fundamental.

[17] The constants in Eq. (3) depend only logarithmically on the important parameters. Thus any reasonable choice of the parameters changes the constants very little.

[18] Similar conclusions are obtained if other expressions for $E_a(\nu_s, T)$ cited in Ref. 15 are used.

[19] Although the crystal displacement also increases by 3 the change is very much smaller than the lengths, $C_3/2f$, being probed.

[20] The lack of a power-level dependence in T_0 also rules out crystal heating as an explanation.

New Microscopic Approach to the Phonon Dispersion in Ionic Crystals

R. Zeyher
Max-Planck-Institut für Festkörperforschung, 7 Stuttgart, Federal Republic of Germany
(Received 7 April 1975)

A microscopic theory of lattice dynamics of ionic crystals is developed in terms of nonorthogonal highly localized wave functions. It is shown that this approach is in close correspondence to some shell models and leads to a microscopic understanding of the model parameters. The phonon dispersion of LiD has been calculated without using any adjustable parameters and it agrees with experiment to within 10% on the average.

The standard approach to microscopic lattice dynamics[1-5] describes the electronic response to core displacements in terms of equilibrium wave functions. As a consequence the dynamical matrix is obtained as a small difference of two large contributions, namely the electrostatic interaction between bare cores and the electronic contribution of the valence electrons. From a computational point of view this cancelation necessitates a very precise evaluation of the electronic part which is difficult to achieve in nonmetals. Several attempts have been made to carry out this cancelation analytically before doing the calculation.[6-8] In the following I propose a different approach which uses localized nonorthogonal orbitals for equilibrium and nonequilibrium configurations. The cancelation problem mentioned above is completely avoided. Moreover this formulation contains a small parameter, namely the overlap of occupied orbitals at different ions, which allows straightforward approximations.

The starting point of the theory is the Hartree-Fock expression for the electronic energy $E(R)$ for a general but fixed ion configuration R,[9]

$$E(R)=2\sum_{n_1,n_2} S_{n_1n_2}{}^{-1}\langle\psi_{n_1}|H_{\text{s.p.}}|\psi_{n_2}\rangle+2\sum_{n_1,n_2,n_3,n_4} S_{n_1n_4}{}^{-1}S_{n_2n_3}{}^{-1}\{2\langle\psi_{n_1}\psi_{n_2}|\psi_{n_3}\psi_{n_4}\rangle-\langle\psi_{n_1}\psi_{n_2}|\psi_{n_4}\psi_{n_3}\rangle\}. \tag{1}$$

The index n denotes both the atom site $\lambda\equiv(l;\kappa)$, where l is a cell and κ an ion index, and the quantum number of occupied orbitals. These orbitals may be nonorthogonal and unnormalized, giving rise to an overlap matrix

$$S_{n_1n_2}=\langle\psi_{n_1}|\psi_{n_2}\rangle . \tag{2}$$

$H_{\text{s.p.}}$ stands for the total electronic Hamiltonian without the Coulomb interaction between electrons. The Coulomb matrix elements are defined by

$$\langle\psi_{n_1}\psi_{n_2}|\psi_{n_3}\psi_{n_4}\rangle=\tfrac{1}{2}e^2\int d^3r_1d^3r_2\psi_{n_1}{}^*(\vec r_1)\psi_{n_2}{}^*(\vec r_2)|\vec r_1-\vec r_2|^{-1}\psi_{n_3}(\vec r_2)\psi_{n_4}(\vec r_1). \tag{3}$$

All quantities in Eq. (1) depend parametrically on the ion configuration R.

The orbitals ψ_n in Eq. (1) are obtained by minimizing the energy $E(R)$. They are well defined even for nonequilibrium configurations though in practice, of course, only the equilibrium functions $\psi_n{}^{(0)}$ can be assumed to be known. To find a reasonable way to calculate the nonequilibrium orbitals ψ_n we note that in ionic crystals the valence electrons are tightly bound to the cores. As a result the orbitals will mainly follow the cores if the cores are displaced. Correspondingly we write

$$\psi_n=\psi_n{}^{(0)}(\vec r-\vec x(\lambda))+\delta\psi_n . \tag{4}$$

The first term in Eq. (4) describes the rigid displacement of $\psi_n{}^{(0)}$ from the equilibrium position $\vec x^{(0)}(\lambda)$ to the general core position $\vec x(\lambda)$. The second term $\delta\psi_n$ takes into account the deformation of this orbital and is at least of first order in the core displacements since it vanishes for the equilibrium configuration.

With use of Eq. (4), Eq. (1) can be written in the following form:

$$E(R)=E^{\text{RI}}(R)+\sum_n\langle\delta\psi_n|V_{nn}|\psi_n{}^{(0)}\rangle+\sum_{n_1,n_2}\langle\delta\psi_{n_1}|W_{n_1n_2}|\delta\psi_{n_2}\rangle . \tag{5}$$

The first term of Eq. (5) summarizes all terms of zeroth order in $\delta\psi_n$, the second term those of first order, and the third term those of second order in $\delta\psi_n$. This defines the operators V_{nn} and $W_{n_1n_2}$. Explicit expressions for these operators within the S^2 approximation[9,10] are obtained if S^{-1} in Eq. (1) is expanded in powers of the overlap of occupied orbitals at different ions up to the second order. We exclude three- and four-center integrals in the following discussion because they are expected to be at least one order of magnitude smaller than the two-center integrals.[10,11]

E^{RI} together with the bare core-core Coulomb contribution contains the electrostatic and short-range repulsive interactions between the ions. These terms lead to a rigid-ion or Kellermann model and should represent the dominant contribution in Eq. (5). E^{RI} together with free-ion functions for $\psi_n{}^{(0)}$ and the S^2 approximation has been used by Löwdin and others[9,10] to calculate lattice constants, cohesive energies, and elastic constants in alkali halides. The second term in Eq. (5) describes the possibility of lowering the interaction energy with neighboring ions by deforming the orbitals. It vanishes for the equilibrium configuration; therefore the first order in the core displacements must be taken. The third term in Eq. (5) corresponds to the increase in energy due to the deformation of the orbitals.

In addition to the rigid-ion term, the Hartree-like matrix elements in the second and third terms in Eq. (5) also give rise to long-range Coulomb interactions among the electrons themselves and between the electrons and cores. The leading long-range parts can be split off by means of a multipole expansion of the Coulomb potentials and the introduction of induced electronic dipole moments on the ions:

$$p_\alpha(\lambda) = -e\sum_n{}' \langle \delta\psi_n | [\vec{r} - \vec{X}(\lambda)]_\alpha | \psi_n^{(0)} \rangle + \text{c.c.} \tag{6}$$

The prime on the summation sign means summation only over occupied states on the ion λ; α is a Cartesian index. When the long-range dipole-dipole interactions are taken out in the second and third terms in Eq. (5), the operators V_{nn} and $W_{n_1n_2}$ become short-range operators $\tilde{V}_{nn}$ and $\tilde{W}_{n_1n_2}$. With neglect of higher-multipole terms, the matrix elements of $\tilde{V}_{nn}$ and $\tilde{W}_{n_1n_2}$ decay exponentially in the two-center approximation.

Let us assume for simplicity that we are dealing with a NaCl lattice and that only longitudinal displacements of the six nearest neighbors contribute to $\tilde{V}_{nn}$. Introducing symmetry coordinates Q^A, $Q_\mu{}^E$, and $Q_\nu{}^T$ for the six longitudinal nearest-neighbor displacements relative to the ion λ ($\mu = 1,2$; $\nu = 1,2,3$; the superscripts A, E, and T indicate $\Gamma_1{}^+$, $\Gamma_{12}{}^+$, and $\Gamma_{15}{}^-$ symmetries, respectively), we write the short-range part of the second term in (5) as

$$Q^A \sum_n{}' \left\langle \delta\psi_n \middle| \frac{\partial \tilde{V}}{\partial Q^A} \middle| \psi_n^{(0)} \right\rangle + \sum_{n,\mu}{}' Q_\mu{}^E \left\langle \delta\psi_n \middle| \frac{\partial \tilde{V}}{\partial Q_\mu{}^E} \middle| \psi_n^{(0)} \right\rangle + \sum_{n,\nu}{}' Q_\nu{}^T \left\langle \delta\psi_n \middle| \frac{\partial \tilde{V}}{\partial Q_\nu{}^T} \middle| \psi_n^{(0)} \right\rangle$$
$$= Q^A \Pi^A + \sum_\mu Q_\mu{}^E \Pi_\mu{}^E + \sum_\nu Q_\nu{}^T \Pi_\nu{}^T. \tag{7}$$

In Eq. (7) the ion index λ and the sum over this index have been omitted. The above defined quantities Π^A, $\Pi_\mu{}^E$, and $\Pi_\nu{}^T$ measure the $\Gamma_1{}^+$, $\Gamma_{12}{}^+$, and $\Gamma_{15}{}^-$ deformations of the ion λ induced by the short-range part of the exciting potential V.

The $\delta\psi_n$'s are obtained by minimizing Eq. (5). By application of the method of Lagrangian multipliers introduced by Tolpygo,[12] this variation is carried out first under the condition that p_ν, Π^A, $\Pi_\mu{}^E$, and $\Pi_\nu{}^T$ remain fixed. One obtains then for the second-order energy after some algebra

$$E^{(2)} = (E^{\mathrm{RI}})^{(2)} + \frac{1}{2} \sum_{\lambda_1 \neq \lambda_2, \nu_1, \nu_2} [P_{\nu_1}(\lambda_1) + p_{\nu_1}(\lambda_1)] C_{\nu_1\nu_2}(\lambda_1\lambda_2) [p_{\nu_2}(\lambda_2) + P_{\nu_2}(\lambda_2)]$$
$$+ \sum_\lambda \left\{ \frac{1}{2}\sum_\nu \frac{p_\nu{}^2(\lambda)}{\alpha(\kappa)} + \frac{1}{2}\sum_\mu \frac{[\Pi_\mu{}^E(\lambda)]^2}{\alpha^E(\kappa)} + \frac{1}{2}\frac{[\Pi^A(\lambda)]^2}{\alpha^A(\kappa)} + \frac{1}{2}\sum_\nu \frac{[Q_\nu{}^T(\lambda)]^2}{\alpha(\kappa)} [\alpha^{-2}(\kappa) - \alpha(\kappa)\alpha^T(\kappa)] \right.$$
$$\left. - \frac{\bar{\alpha}(\kappa)}{\alpha^T(\kappa)} \sum_\nu Q_\nu{}^T(\lambda) p_\nu(\lambda) - \Pi^A(\lambda) Q^A(\lambda) - \sum_\mu \Pi_\mu{}^E(\lambda) Q_\mu{}^E(\lambda) \right\}. \tag{8}$$

$P_\nu(\lambda)$ is the ionic dipole moment and C the Coulomb-force-constant matrix. α, α^A, α^E, α^T, and $\bar{\alpha}$ are coupled Hartree-Fock polarizabilities[13] associated with the operators $[\vec{X} - \vec{X}(\lambda)]_\nu$, $\partial\tilde{V}/\partial Q^A$, $\partial\tilde{V}/\partial Q_\mu{}^E$, $\partial\tilde{V}/\partial Q_\nu{}^T$, and the mixed combination of $[\vec{X} - \vec{X}(\lambda)]_\nu$ and $\partial\tilde{V}/\partial Q_\nu{}^T$, respectively. In a second step $E^{(2)}$ is minimized also with respect to p_ν, Π^A, $\Pi_\mu{}^E$, and $\Pi_\nu{}^T$ which allows the elimination of these coordinates.

With neglect of the fourth term in the curly brackets, Eq. (8) is equivalent to a phenomenological shell model in which the shells simulate $\Gamma_1{}^+$-, $\Gamma_{12}{}^+$-, and $\Gamma_{15}{}^-$-like deformations of the ions. With omission of the quadrupolar deformation, a term by term comparison with the work of Schröder[14] gives the following relations:

$$\frac{y^2(\kappa)}{g^T(\kappa)} = \alpha(\kappa); \quad \frac{y(\kappa)}{A} = -\frac{\alpha(\kappa)}{\sqrt{2}\,\bar{\alpha}(\kappa)}; \qquad \frac{3}{2}\frac{A^2}{g^A(\kappa)} = \alpha^A(\kappa). \tag{9}$$

The left-hand sides in Eq. (9) contain model parameters; the right-hand sides, the equivalent microscopic quantities. y denotes the shell charge and g^A and g^T the intra-ionic shell-core springs for the breathing and the dipolar deformation. The transverse spring constant B in the polarization part of the shell model of Ref. 14 has been put equal to zero, corresponding to the neglect of all transverse contributions to $\tilde{V}$ in the microscopic theory. Equations (8) and (9) give the phenomenological shell models a quantum mechanical foundation, and especially the shell charge a precise meaning.

I have carried out numerical calculations for LiD to test the above theory. Each of the orbitals $\psi_n^{(0)}$ was represented by a linear combination of two Gaussian functions,

$$\psi_n^{(0)}(\vec{r}) = \sum_{\nu=1}^{2} a_\nu(\kappa) \exp[-b_\nu(\kappa) |\vec{r} - \vec{X}(\lambda)|^2].$$

Minimization of the energy $E(R^{(0)})$ determined the constants a_ν and b_ν and yielded a theoretical lattice constant of $a = 4.34$ Å in rough agreement

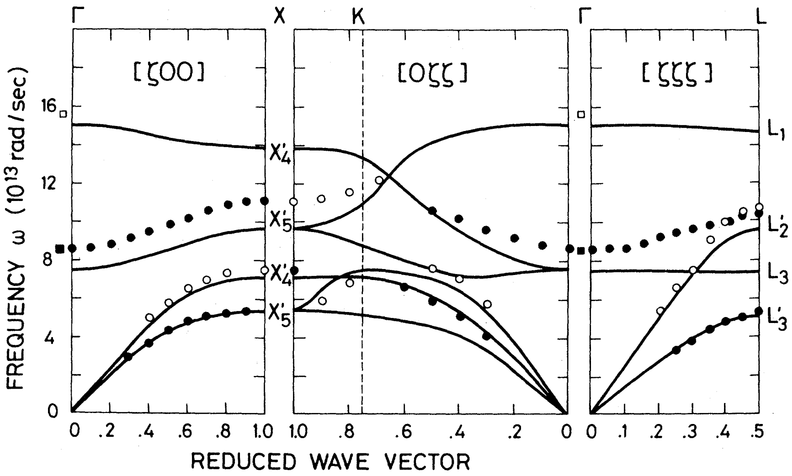

FIG. 1. The solid lines are the calculated phonon dispersion curves in ^{7}LiD. The open and closed circles and squares are experimental points at 300 K (Ref. 15).

with the experimental value 4.10 Å. Using these orbitals I obtained the following values for the repulsive force constants in units of $2e^2/a^3$: $A = 8.22$, $B = -0.97$, $A' = 0.40$, and $B' = -0.09$. Finally the five polarizabilities of the D$^-$ ion have been determined by means of a variational procedure. For the Γ_1^+ deformation I used the orbitals $\psi_n^{(0)}$ and calculated the relaxation of the constants a_ν and b_ν due to the Γ_1^+ displacement of the nearest neighbors. For the Γ_{15}^- deformation $\delta\psi$ was represented by two Gaussian orbitals with opposite signs which were slightly displaced from the D$^-$ core to obtain z-like behavior. The free constants again were determined by minimization of the electronic energy after turning on the various Γ_{15}^- perturbations. The Γ_{12}^+ deformation was determined in a similar way and turned out to be negligible compared to the Γ_1^+ deformation. Expressing the various polarizabilities in terms of the more familiar spring constants by means of Eq. (9), I obtained the values $y = -0.73e$, $g^A = 26.2$, and $g^T = 15.0$. Using the above values I calculated the phonon dispersion in LiD along the symmetry directions. The solid lines in Fig. 1 represent the theoretical dispersion curves; the open and closed circles and squares are experimental points for longitudinal and transverse phonons at room temperature.[15]

In conclusion I have presented a no-parameter microscopic theory for the lattice dynamics of ionic crystals which seems to be better suited for numerical calculations than the other microscopic theories. As an example I have applied it to LiD and found the lattice constant and the acoustical branches in agreement with experiment within 5%. The optical branches show larger discrepancies with a maximum error of 25% in the TO branch at the L point.

It is a pleasure to thank Professor H. Bilz, Professor S. S. Jaswal, Dr. W. Hanke, and Dr. W. Weber for helpful comments.

---

[1] L. J. Sham, Phys. Rev. 188, 1431 (1969).

[2] R. M. Pick, M. H. Cohen, and R. M. Martin, Phys. Rev. B 1, 910 (1970).

[3] N. Wakabayashi and S. K. Sinha, Phys. Rev. B 10, 745 (1974).

[4] C. M. Bertoni, V. Bortolani, C. Calandra, and E. Tosatti, Phys. Rev. B 9, 1710 (1974).

[5] B. Gliss and H. Bilz, Phys. Rev. Lett. 21, 884 (1968).

[6] S. K. Sinha, Phys. Rev. 177, 1256 (1969).

[7] R. M. Pick, in *Elementary Excitations in Solids, Molecules, and Atoms*, edited by J. T. Devreese, A. B. Kunz, and T. C. Collins (Plenum, New York, 1973), Pt. B, p. 25.

[8] H. Eschrig, Phys. Status Solidi (b) 56, 197 (1973).

[9] P. O. Löwdin, Advan. Phys. 5, 1 (1956).

[10] I. V. Abarenkov and I. M. Antonova, Phys. Status Solidi 38, 783 (1970).

[11] R. Zeyher, Phys. Status Solidi (b) 48, 711 (1971).

[12] K. B. Tolpygo, Fiz. Tverd. Tela 3, 943 (1961) [Sov. Phys. Solid. State 3, 685 (1961)].

[13] A. Dalgarno, Advan. Phys. 11, 281 (1962).

[14] U. Schröder, Solid State Commun. 4, 327 (1966).

[15] J. L. Verble, J. L. Warren, and J. L. Yarnell, Phys. Rev. 168, 980 (1968).